PCCP

Dynamic Article Links

Cite this: *Phys. Chem. Chem. Phys.*, 2011, **13**, 1434–1439

www.rsc.org/pccp

PAPER

Drainage of the air–water–quartz film: experiments and theory

Rogerio Manica*[a] and Derek Y. C. Chan[abc]

Received 25th May 2010, Accepted 5th November 2010
DOI: 10.1039/c0cp00677g

Experimental results of the kinetics of drainage of the trapped water film between an approaching air bubble and a quartz plate have been analysed using recent theoretical advances in formulating and solving the flow problem in deformable films. Excellent agreement is obtained between experimental data and a model that assumes the bubble–water interface is tangentially immobile in its hydrodynamic response. The coupling between hydrodynamic pressure, disjoining pressure and film deformation is critical in determining the dynamic behaviour of the drainage process. The Reynolds parallel film model that omits the effects of film deformation predicts results that are qualitatively incorrect.

1. Introduction

The dynamics of the interaction between a solid surface and a deformable drop or bubble in water and the associated problem of the drainage of the entrapped water film is a fundamental process that occurs in many technical applications. These range from the optimisation of mineral flotation efficiency to the efficacy of ultrasonic contrasting agents to the transport of soft matter in microfluidic cells.

The first successful measurement of the spatial and temporal evolution of a draining aqueous film between a bubble and a smooth hydrophilic quartz plate was made almost two decades ago by Fisher *et al.*[1–3] They pointed out particular challenges of such experiments because it was "very difficult to compare results from different laboratories, since the method of forming the draining film profoundly affects its shape and the kinetics of the evolution of that shape. It is by no means clear that all authors publishing in the field have been aware of these limitations." They further noted a "scarcity of data where the initial conditions for film formation have been reliably and reproducibly controlled". These comments still apply today as the only studies of the spatial and temporal deformations of thin films are those by Horn *et al.* on the dynamic deformations of a mercury drop[4–6] and a bubble[7] approaching a mica plate and by Klaseboer *et al.*[8,9] on the deformations of two approaching drops in another liquid.

Although the governing equations for film drainage involving deformable boundaries have been formulated for some time, it was only recently that boundary conditions appropriate to different experimental conditions have been developed[10,11] to provide the key to practical implementation of numerical solutions. In particular, it became relatively easy to account accurately for the vastly different intrinsic length scales of the problem: nanometre for the film thickness, micrometre for the deformed region of the film and millimetre for the drop or bubble size.

In this paper we analyse the film drainage data of Fisher *et al.* using recent advances in modelling time-dependent interactions between deformable drops and bubbles. In doing so, we

(a) determine the hydrodynamic boundary condition that must prevail at the bubble–water interface,

(b) demonstrate the importance of bubble deformation in giving a quantitative account of the drainage kinetics, and

(c) determine the shortcomings of the commonly accepted Reynolds parallel film model for film drainage in its failure to predict the correct quantitative effects of disjoining pressure on the rate of drainage of deformable films.

We begin with a brief summary of the experimental approach of Fisher *et al.* in Section 2 and develop the theoretical model that will be used to analyse the film drainage data in Section 3. Detailed comparisons between experiments and theory are given in Section 4 and conclusions are summarised in the final section.

2. Experimental method

Here we only give a brief summary of how a draining film of distilled water or an aqueous electrolyte of known concentration of sodium chloride was formed between an air bubble and an optically polished (to 0.1 wavelength) hydrophilic quartz plate. The original papers by Fisher *et al.*[1–3] should be consulted for further details.

As the initial step, a static protuberant air bubble of radius R_o = 1.16 mm and an apical height of 570 μm was created at a

[a] *Institute of High Performance Computing, 1 Fusionopolis Way, 138632, Singapore. E-mail: manicar@ihpc.a-star.edu.sg; Fax: +65 6463 0200; Tel: +65 6419 1111*
[b] *Department of Mathematics & Statistics, The University of Melbourne, Parkville, Victoria 3010, Australia. E-mail: D.Chan@unimelb.edu.au; Fax: +61 3 8344 4599; Tel: +61 3 8344 5556*
[c] *Department of Mathematics, National University of Singapore, 117543, Singapore*

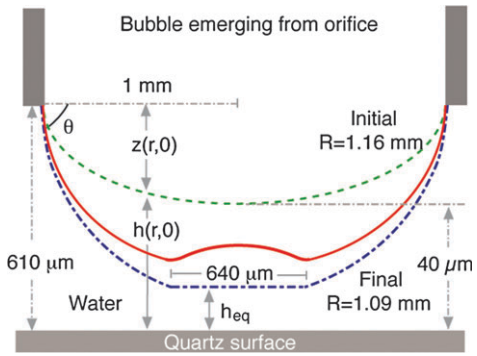

Fig. 1 A schematic diagram (not to scale) of the experimental configuration of a protuberant bubble in an aqueous electrolyte against a quartz plate that depicts the initial, transient and final states of the bubble.

2 mm diameter orifice in a Kel-F chamber. The quartz plate is positioned 40 μm from the apex of the bubble and optical alignment was carried out to ensure axial symmetry (Fig. 1). The Laplace pressure of the bubble was thus estimated to be $P_{init} = 124$ Pa.

The drainage experiment began by activating a spring-loaded lever that rapidly compressed a section of the sealed air line supplying the bubble over a very brief period of much less than 1 s. This produced an expanded bubble that flattened at the apex against the quartz plate trapping an intervening draining film of diameter $2a = 640$ μm. From the geometry of the experimental setup, see Fig. 1, the radius of the expanded bubble, approximated by a truncated sphere, was estimated to be $R = 1.09$ mm, corresponding to a final Laplace pressure, $P_{final} = 132$ Pa. Thus the total force, F, acting on the deformed bubble can be estimated as $F \approx (\pi a^2)P_{final} \approx 43$ μN.

Reproducibility of this method of bubble expansion was very high and was a key feature of this experimental approach.

Time-variations of the intensity of a He–Ne laser beam reflected from a given radial position, r, gave the time evolution of the film thickness, $h(r,t)$, at that point. By repeating such measurements at different r positions with similarly created bubbles allowed the entire spatial–temporal variation of film thickness to be mapped. Spatial resolution was limited by the laser beam of diameter $\sim$30 μm.

Data for the film profile from 5 s after bubble expansion were recorded for over 200 s as film drainage proceeded. Such data sets were used in our analysis.

3. Theory

The slow hydrodynamic drainage of the axisymmetric water film trapped between the bubble and the quartz can be described by the lubrication theory in the Stokes flow. The film thickness, $h(r,t)$, is a function of the radial position, r, and time, t, while the hydrodynamic pressure, $p(r,t)$ in the film, measured relative to the pressure in the bulk fluid, only varies in the radial direction. The dominant fluid velocity component, $u(z,t)$, is in the radial direction and depends on the coordinate, z, normal to the quartz plate.

On the quartz surface at $z = 0$, the familiar no-slip boundary condition is assumed to hold at a fluid–solid interface so the fluid velocity vanishes: $u(0,t) = 0$. At the bubble surface, $z = h(r,t)$, one can either assume the tangentially immobile boundary condition: $u(h,t) = 0$ or the fully mobile, zero tangential stress condition: $\partial u/\partial z = 0$. Other possible boundary conditions that attempt to include effects due to surface elasticity or an interfacial surfactant layer lie between these limits.

With this model, the film thickness, h, and the pressure, p, are related by the Stokes–Reynolds equation[12]

$$\frac{\partial h}{\partial t} = \frac{\beta}{12\mu r}\frac{\partial}{\partial r}\left(rh^3\frac{\partial p}{\partial r}\right) \qquad (3.1)$$

where μ is the dynamic viscosity of the aqueous solution. For the tangentially immobile condition at the bubble–water interface, the constant $\beta = 1$, while the mobile, zero tangential stress boundary condition corresponds to $\beta = 4$.

Deformation of the bubble–water interface with a constant interfacial tension σ is given by the Young–Laplace equation[12]

$$\frac{\sigma}{r}\frac{\partial}{\partial r}\left(r\frac{\partial h}{\partial r}\right) = \frac{2\sigma}{R} - \Pi - p \qquad (3.2)$$

where $\Pi(h(r,t))$ is the disjoining pressure due, for example, to electrical double layer and van der Waals interactions between the quartz plate and the bubble–water interface: $\Pi > 0$ corresponds to repulsion. In the present experiment with NaCl concentrations below 1 mM and in the range of film thickness in these experiments, it can be shown that Π is entirely due to repulsive electrical double layer interactions. The magnitude of van der Waals interaction is negligibly small. For later reference we call eqn (3.1) and (3.2) the Stokes–Reynolds–Young–Laplace (SRYL) equations.

To solve the SRYL equations, we need to specify the initial shape and velocity of the bubble together with boundary conditions that describe the expanding bubble experiment. We will develop these conditions in detail in Section 3.2 where we will describe how to model the film drainage experiments by solving the SRYL equations.

The challenge of having to solve the SRYL equations as a pair of coupled partial differential equations has led to the development of a number of approximate solutions to the problem. Many of the simpler models have shown to be unsuitable for providing quantitative descriptions of the present experimental results.[3]

The Reynolds parallel film model, developed independently by Stefan and Reynolds,[13] is often used as an approximate solution of the SRYL equations. It has been applied to describe time dependent interactions involving bubbles and drops[14] and a number of complex extensions to the model have been proposed.[15] The availability of such detailed experimental data for the spatial and temporal evolution of a draining water film between a well-characterised system of bubble and a quartz plate provides an ideal opportunity to examine the predictions of the Reynolds parallel film model compared to the solution of the SRYL equations.

3.1 Reynolds parallel film model

The Reynolds parallel film (RPF) model assumes that the water film between the bubble and the quartz plate has

uniform thickness, $h(t)$, so that the bubble–water interface is regarded as a disk of fixed radius a in the radial direction. However, the magnitude of the film radius, a, is not known *a priori*. Since the film is assumed to remain flat during the drainage process, the Young–Laplace equation (eqn (3.2)) that describes film deformation is no longer required. With the film thickness, $h(t)$, now being independent of r, the Stokes–Reynolds equation (eqn (3.1)) can be integrated with the boundary condition $p(a,t) = 0$ to give

$$p(r,t) = -\frac{3\mu}{\beta h^3}\left(\frac{\mathrm{d}h}{\mathrm{d}t}\right)(a^2 - r^2). \tag{3.3}$$

The hydrodynamic force, F_{hy} in the z direction, due to viscous film drainage arising from this pressure distribution is

$$F_{\mathrm{hy}} = 2\pi\int_0^a p(r,t)r\mathrm{d}r = -\frac{3\pi\mu a^4}{2\beta h^3}\left(\frac{\mathrm{d}h}{\mathrm{d}t}\right) \tag{3.4}$$

where hydrodynamic repulsion corresponds to $F_{\mathrm{hy}} > 0$. By balancing the applied force, $F_{\mathrm{app}} > 0$, that drives the bubble towards the quartz plate against the hydrodynamic force, F_{hy}, and the force due to disjoining pressure, $\Pi(h)(\pi a^2)$, we obtain an expression for the rate of drainage

$$\frac{\mathrm{d}h}{\mathrm{d}t} = -\frac{2\beta h^3}{3\pi\mu a^4}[F_{\mathrm{app}} - \Pi(h)(\pi a^2)]. \tag{3.5}$$

This result shows that according to the Reynolds parallel film model a repulsive disjoining pressure, $\Pi(h) > 0$, will retard the rate of drainage. We will show that this is opposite to what is observed in the bubble–quartz experiment and the predictions of the SRYL model using eqn (3.1) and (3.2).

Furthermore, if the disjoining pressure is due to van der Waals attraction of the form: $\Pi(h) = -A/(6\pi h^3)$, eqn (3.5) can be solved analytically to give a finite coalescence time.[14] Therefore it is not necessary to invoke the concept of surface waves as a trigger for coalescence.[15,16]

3.2 Boundary conditions for film drainage

In this section we develop the initial and boundary conditions that are appropriate to describe the bubble expansion and film drainage experiment of Fisher *et al.*[1–3] For an axisymmetric film, we have the boundary conditions: $\partial h/\partial r = 0 = \partial p/\partial r$ at $r = 0$ that follows from symmetry and $p \to 0$ as $r \to \infty$. As described in the previous section, the initial distance of closest approach in the experiment, h_{o} (40 μm), between the bubble and the quartz plate is much smaller than the drop radius, R_{o} (1.16 mm). The initial shape of the film can be represented accurately by a parabolic profile: $h(r,t = 0) = h_{\mathrm{o}} + r^2/(2R_{\mathrm{o}})$.

After the rapid expansion of the bubble by triggering the spring-loaded lever to compress the air line and drive the bubble towards the quartz plate at $t = 0$, the first experimental observation was taken at around $t \approx 0.5$ s when the film was observed to have already developed a dimple. There were no experimental data reported for $t < 0.5$ s. It was observed that the drainage kinetics of the film shape between 5 to 200 s was very reproducible. All this suggests that transient effects associated with the bubble expansion process in the initial 0.5 s had totally dissipated and the film drained under a constant force condition during the measurement period. Consequently, in modelling this experiment, the details of how the initial rapid bubble expansion is achieved are not critical and indeed the event is so rapid that measurements were not possible. The key therefore is to construct a simple model for this initial rapid expansion to obtain the correct shape of the film that was measured at the first time point at 5 s and then predict how the shape of the film evolved for a further 200 s.

The analysis of the transient deformation kinetics of an anchored mercury drop in water due to a mica plate that was driven momentarily towards it revealed a similar response to the bubble–quartz experiment.[17] The drop formed a dimple in response to the approaching mica plate and after the mica had stopped moving, the deformed mercury–water interface continued to evolve while the force acting on the drop remained constant. In the mercury drop experiment, we model the momentary approach of the mica plate during the brief period $0 < t < t_{\mathrm{o}}$ by imposing the following condition at the boundary of the domain $0 < r < r_{\max}$ in which we solve the SRYL equations:[11]

$$\frac{\partial h(r_{\max},t)}{\partial t} + \frac{\alpha}{2\pi\sigma}\frac{\mathrm{d}F(t)}{\mathrm{d}t} + U(t) = 0 \tag{3.6}$$

where $F(t)$ is the total force acting on the bubble given by

$$F(t) = 2\pi\int_0^\infty [p(r,t) + \Pi(h(r,t))]r\mathrm{d}r \tag{3.7}$$

In the mercury–mica experiment the function $U(t)$ could be estimated from experimental conditions. It turned out that the most important feature in modelling the experiment is the total distance, X, travelled during this initial period:

$$X = \int_0^{t_{\mathrm{o}}} U(t)\mathrm{d}t \tag{3.8}$$

rather than the detailed form of $U(t)$ because the final deformation is determined by the total displacement X.

In modelling the very rapid initial expansion in the present bubble experiment we choose $U(t)$ to have the form

$$U(t) = \begin{cases} U_{\mathrm{o}}, & 0 < t < t_{\mathrm{o}} \\ 0, & t_{\mathrm{o}} < t \end{cases} \tag{3.9}$$

Table 1 Experimental parameters for the results in Fig. 2

	Fig. 2a[1,2]	Fig. 2b[3]	Fig. 2c[3]
Initial radius/mm	1.16	1.16	1.16
Final radius/mm	1.09	1.11	1.11
Initial separation/μm	40	40	40
Rim radius/μm	320	200	200
Velocity, U_{o}/mm s^{-1}	2.75	2.75	2.75
Approach time, t_{o}/s	0.055	0.04	0.036
Surface potential—bubble/mV^3	−34	−34	−34
Surface potential—quartz/mV^3	−148	−130	−122
Concentration/mM	2×10^{-3}	0.25	1
Contact angle	67°	64°	64°
Surface tension/mN m^{-1}	72.8	72.8	72.8
Viscosity/Pa s	0.89	0.89	0.89

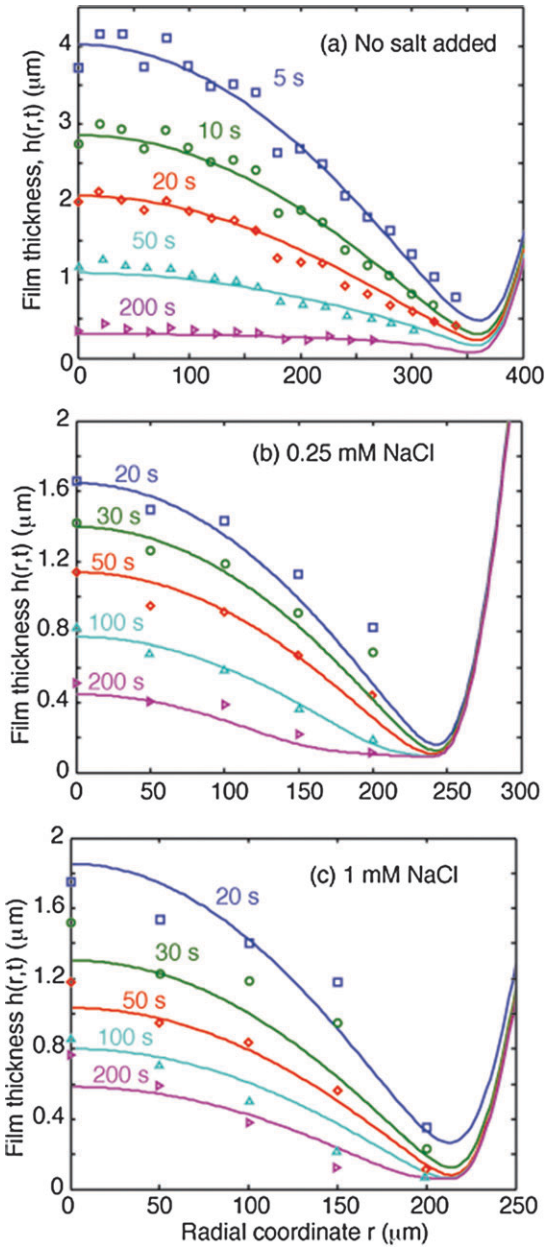

Fig. 2 Shape of the draining water film between a bubble and a quartz plate in (a) distilled water (taken to have $\sim 2 \times 10^{-6}$ mM NaCl), (b) 0.25 mM NaCl and (c) 1 mM NaCl.

so that $X = U_o t_o$. In modelling all experiments, we have taken $U_o = 2.75$ mm s^{-1} and chose the value of t_o to give the correct film shape at $t = 5$ s. The values of t_o are small (<0.1 s) and varied slightly between experiments, see Table 1.

During this initial expansion period and throughout the experiment, the bubble is pinned to the orifice of radius 1 mm (see Fig. 1). When the bubble is so pinned, the quantity α in eqn (3.6) has the form[11]

$$\alpha \equiv 1 + \ln\left(\frac{r_{max}}{2R_o}\right) + \tfrac{1}{2}\ln\left(\frac{1+\cos\theta}{1-\cos\theta}\right) \qquad (3.10)$$

where θ is the initial angle that the bubble makes with the orifice before the expansion takes place (see Fig. 1). Although the contact angle must change during the expansion stage, the expressions in eqn (3.6) and (3.10) have already taken this into account.[11] The assumption here is that the deformation zone is small compared to the dimensions of the bubble and that the deforming bubble is to a very good approximation regarded as incompressible.[11]

An alternative is to model this initial expansion in the first ~ 0.1 s by using a force ramp instead of the velocity ramp in eqn (3.9) to create the first measured film profile taken at 5 s. As we observed above the detailed method of the brief expansion process in the initial ~ 0.1 s does not affect the drainage process that was measured between 5–200 s. The key is to ensure the initial shape at 5 s is correct.

The form of $U(t)$ that drives the initial expansion in the boundary condition, eqn (3.9), encapsulates the mechanical phenomenon of fast bubble expansion. As we shall see, we can use the same function to model different drainage experiments under different aqueous electrolyte concentrations. This lends further support to our notion that the details of this initial transient of bubble expansion that extends over <0.1 s are not critical to the modelling and understanding of the film drainage process that takes place over 200 s.

The SRYL equations together with the initial and boundary conditions developed in this section form a differential algebraic equation system that can be solved by the method of lines using standard numerical packages such as ode15s in Matlab. Details of the numerical methods have been given elsewhere.[10,11]

4. Results and discussions

In order to compare the results of the SRYL model with results from drainage experiments of a bubble against a quartz plate, we need to specify the form of the disjoining pressure $\Pi(h)$. As experimental results are all taken at concentrations of 1 mM NaCl or less, electrical double layer repulsion provides the only significant contribution to the disjoining pressure. The magnitude of van der Waals interaction is negligible in this regime. Relevant physical parameters such as surface potentials and interfacial tensions are taken from Fisher *et al.* These are summarised in Table 1.

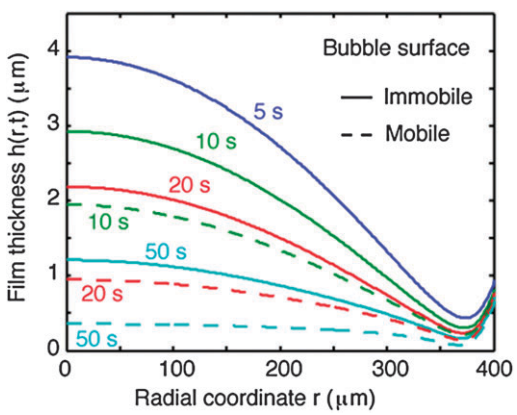

Fig. 3 Effects of the hydrodynamic boundary condition at the bubble surface on film drainage.

In Fig. 2, we compare the evolution of the film thickness measured in distilled water (taken to have 2×10^{-6} M NaCl),[18] in 0.25 mM and in 1 mM NaCl with corresponding predictions of the SRYL model under the tangentially immobile boundary condition at the bubble–water interface: $\beta = 1$ in eqn (3.1). After the profile at the earliest time step has been used to determine the drive velocity function $U(t)$ in eqn (3.9), there are no other free parameters in the model. The agreement between experiment and theory in Fig. 2 is very good.

We note that at earlier time, $t \approx 20$ s, the films have a well-defined dimple of radius r_{rim}, and the film thickness varied by over a factor of 4 between the centre and r_{rim}. The slight variations in the dimple radius across Fig. 2a–c are likely to be due to the slightly differing amounts of air used in inflating the bubbles.

The faster drainage rate that results from using the zero tangential stress, fully mobile boundary condition ($\beta = 4$) at the bubble–water interface instead of the tangentially immobile condition ($\beta = 1$) can be seen in Fig. 3. For this illustration, we take as the initial condition the film shape in distilled water ($\sim 2 \times 10^{-6}$ M NaCl) (Fig. 2a) at 5 s and calculate how the film will evolve subsequently under the two different boundary conditions at the bubble surface. However, the magnitude of the electrical double layer repulsion that controls the thickness of the film at r_{rim} also affects the rate of thinning of the film. This is the reason why the difference in the drainage rate between the tangentially immobile and mobile boundary conditions at the bubble surface is not a simple factor of 4.

The observation that the tangentially immobile boundary condition on the bubble surface afforded good agreement with the cases of film drainage considered here is consistent with atomic force microscope measurements. Results and features of the force between the microbubble (~ 100 μm diameter) that has been driven towards a mica plate[19] and the force between two colliding bubbles that lead to bubble coalescence on separation[20] can only be accounted for by the immobile boundary condition on the bubble surfaces.

We can also compare changes in the volumetric drainage rate that arise from a disjoining pressure, Π, due to electrical double layer repulsion. In the SRYL model, we define the volume of water trapped at any time between the dimpled bubble surface and the quartz plate by

$$V_{SRYL}(t, \Pi) = 2\pi \int_0^{r_{rim}} h(r, t) r \mathrm{d}r \qquad (4.1)$$

For the Reynolds parallel film (RPF) model, we can identify the disk radius a with r_{rim} and the volume of water in the film is simply $V_{RPF}(t,\Pi) = (\pi a^2 h)$. In Fig. 4, we compare the time variation of the ratio of the volume of water in the film in the absence of a disjoining pressure, $V(t,0)$, to that in the presence of a repulsive disjoining pressure, $V(t,\Pi)$, corresponding to electrical double layer repulsion in distilled water.

The SRYL model predicts that in the presence of a repulsive disjoining pressure, the film will drain *faster*, that is the ratio: $V(t,0)/V(t,\Pi) > 1$ (Fig. 4). The reason for this is that the film thickness at the rim radius r_{rim} is the key parameter that controls the film drainage rate. A repulsive disjoining pressure, $\Pi(h)$, serves to keep the film thicker at r_{rim} for longer and thus facilitates faster film drainage through this bottleneck.

On the other hand, with the Reynolds parallel film model, the bubble–water interface is assumed to be flat and non-deformable. As a result of ignoring film deformation, this model predicts that drainage will become *slower*, that is the ratio: $V(t,0)/V(t,\Pi) < 1$, in the presence of a repulsive disjoining pressure (Fig. 4). The observed trend in the bubble–quartz experiment is in agreement with the SRYL model but is opposite to that predicted by the Reynolds parallel film model.

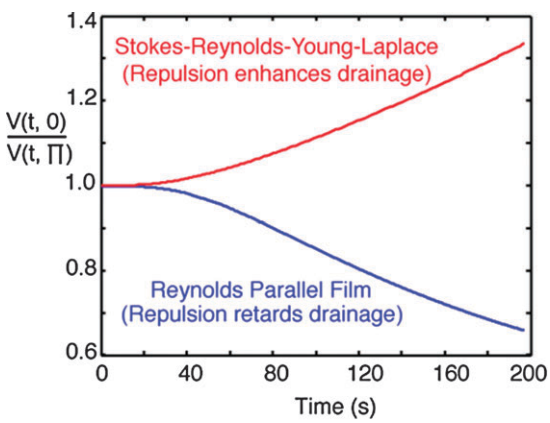

Fig. 4 Comparison of relative changes in film volume with drainage time in the absence and presence of a repulsive disjoining pressure Π according to the Stokes–Reynolds–Young–Laplace model and the Reynolds parallel film model.

5. Conclusions

Using recent theoretical advances in the modelling of time dependent forces between interacting deformable drops and bubbles we are able to undertake a quantitative analysis of data acquired about the kinetics of film drainage between a bubble and a quartz plate. The experimental results are consistent with a model of thin film hydrodynamic lubrication flow where the bubble–water interface behaves as a tangentially immobile boundary rather than an earlier model that assumed mobile interfaces.[21] Although the precise reason why the bubble–water interface (even for distilled water) appears to be immobile rather than mobile is not clear, it is known that trace amounts of surface active agents, at concentrations that will reduce the interfacial tension by about 0.1 mN m^{-1}, will be sufficient to arrest surface mobility and result in an immobile surface.[22]

The need to include effects due to surface deformations during film drainage is vital in accounting for the precise spatial and temporal evolution of the draining film. Therefore simple models such as the Reynolds parallel film and its variants that neglect deformation fail to even predict the qualitative trend of the effect of repulsive disjoining pressure on the volumetric drainage rate.

Our success in analysing the well-characterised experiments of the drainage of an aqueous film between a bubble and a quartz plate suggests that we have a reliable foundation to understand complex time-dependent interactions involving

deformable soft materials. The model has also been applied to demonstrate analytically that as a result of deformation, bubbles or drops can be triggered to coalesce by separating them rather than by forcing them together[23,24] as observed experimentally.[25,26]

This work is supported in part by the Australian Research Council through the Discovery Project Scheme. DYCC is a Visiting Scientist at the Institute of High Performance Computing and an Adjunct Professor at the National University of Singapore.

Notes and references

1 L. R. Fisher, E. E. Mitchell, D. Hewitt, J. Ralston and J. Wolfe, *Colloids Surf*., 1991, **52**, 163.
2 L. R. Fisher, D. Hewitt, E. E. Mitchell, J. Ralston and J. Wolfe, *Adv. Colloid Interface Sci*., 1992, **39**, 397.
3 D. Hewitt, D. Fornasiero, J. Ralston and L. R. Fisher, *J. Chem. Soc., Faraday Trans*., 1993, **89**, 817.
4 J. N. Connor and R. G. Horn, *Faraday Discuss*., 2003, **123**, 193.
5 L. Y. Clasohm, J. N. Connor, O. I. Vinogradova and R. G. Horn, *Langmuir*, 2005, **21**, 8243.
6 R. Manica, J. N. Connor, L. Y. Clasohm, S. L. Carnie, R. G. Horn and D. Y. C. Chan, *Langmuir*, 2008, **24**, 1382.
7 R. A. Pushkarova and R. G. Horn, *Langmuir*, 2008, **24**, 8726.
8 E. Klaseboer, J. Ph. Chevaillier, C. Gourdon and O. Masbernat, *J. Colloid Interface Sci*., 2000, **229**, 274.
9 R. Manica, E. Klaseboer and D. Y. C. Chan, *Soft Matter*, 2008, **4**, 1613.
10 S. L. Carnie, D. Y. C. Chan, C. Lewis, R. Manica and R. R. Dagastine, *Langmuir*, 2005, **21**, 2912.
11 R. Manica, J. N. Connor, R. R. Dagastine, S. L. Carnie, R. G. Horn and D. Y. C. Chan, *Phys. Fluids*, 2008, **20**, 032101.
12 C. Y. Lin and J. C. Slattery, *AIChE J*., 1982, **28**, 147.
13 J. Stefan, *Sitzungsber. Akad. Wiss. Wien, Math.-Naturwiss. Kl., Abt. 2A*, 1874, **69**, 713; O. Reynolds, *Philos. Trans. R. Soc. London*, 1886, **177A**, 157.
14 S. A. K. Jeelani and S. Hartland, *J. Colloid Interface Sci*., 1993, **156**, 467.
15 I. B. Ivanov and P. A. Kralchevsky, *Colloids Surf., A*, 1997, **128**, 155; *Thin liquid films fundamentals and applications*, Surfactant Science Series, ed. I. B. Ivanov, M. Dekker, 1988, vol. 29.
16 A. Vrij, *Discuss. Faraday Soc*., 1966, **42**, 23.
17 R. Manica, J. N. Connor, S. L. Carnie, R. G. Horn and D. Y. C. Chan, *Langmuir*, 2007, **23**, 626.
18 R. Manica, L. Parkinson, J. Ralston and D. Y. C. Chan, *J. Phys. Chem. C*, 2010, **114**, 1942.
19 O. Manor, I. U. Vakarelski, X. Tang, S. J. O'Shea, G. W. Stevens, F. Grieser, R. R. Dagastine and D. Y. C. Chan, *Phys. Rev. Lett*., 2008, **101**, 024501.
20 I. U. Vakarelski, R. Manica, X. Tang, S. J. O'Shea, G. W. Stevens, F. Grieser, R. R. Dagastine and D. Y. C. Chan, *Proc. Natl. Acad. Sci. U. S. A*., 2010, **107**, 11177.
21 S. G. Yiantsios and R. H. Davis, *J. Fluid Mech*., 1990, **217**, 547.
22 O. Manor, I. U. Vakarelski, G. W. Stevens, F. Grieser, R. R. Dagastine and D. Y. C. Chan, *Langmuir*, 2008, **24**, 11533.
23 D. Y. C. Chan, E. Klaseboer and R. Manica, *Soft Matter*, 2009, **5**, 2858.
24 D. Y.C. Chan, E. Klaseboer and R. Manica, *Soft Matter*, 2010, **6**, 1809.
25 N. Bremond, A. R. Thiam and J. Bibette, *Phys. Rev. Lett*., 2008, **100**, 024501.
26 D. Z. Gunes, X. Clain, O. Breton, G. Mayor and A. S. Burbidge, *J. Colloid Interface Sci*., 2010, **343**, 79.